Earthq Eng & Eng Vib (2015) 14: 411-421 **DOI**:10.1007/s11803-015-0033-2

Investigation into dynamic response of regional sites to seismic waves using shaking table testing

Li Yadong[1†], Cui Jie[1,2‡], Guan Tianding[1,2†] and Jing Liping[3‡]

1. *School of Civil Engineering, Guangzhou University, Guangzhou 510006, China*
2. *Earthquake Engineering Research& Test Center, Guangzhou University, Guangzhou 510405, China*
3. *Key Laboratory of Earthquake Engineering and Engineering Vibration*, *Institute of Engineering Mechanics, China Earthquake Administration, Harbin 150080, China*

Abstract: This study addresses the changes in acceleration, pore water pressure and Fourier spectrums of different types of seismic waves with various amplitudes via large-scale shaking table tests from two sites: a sand-containing regional site and an all-clay site. Comparative analyses of the test results show that the pore water pressures in sand-soil layers of the regional site initially increase and then decrease as the amplitudes of the seismic accelerations increase. The actions of the vertical and vibrational seismic waves contribute to greater pore water pressures. The amplification coefficient of the sand-layer regional site becomes smaller as the seismic waves grow stronger, so that both sites are capable of filtering high frequencies and amplifying low frequencies of seismic waves. This is more apparent with the increase in the peak value of the acceleration, and the natural vibration frequencies of both sites decrease with the transmission of the seismic waves from the basement to the ground surface. The decreasing frequency value of the sand-containing regional site is smaller than that of the all-clay site.

Keywords: shaking table test; regional site; all-clay site; seismic dynamic response; acceleration analysis; spectrum analysis

1 Introduction

From shaking table tests and analyses of the response to seismic waves that have been achieved in recent years, it is known that local sites conditions have great influence on seismic transmission, which can affect the extent of casualties and injuries, as well as severe damage to the built environment.

Due to the differences in forming age and genetic types, the dynamic characteristics of soil layers show significant nonuniformity, which is distributed throughout naturally forming soil and shows its own law and regionality. Site soil conditions are important factors to be taken into account in designing aseismic buildings, and it is necessary to probe further into the dynamic characteristics of a regional site under the action of seismic waves.

The dynamic responses of many regional sites have been widely studied. For example, Li (1992) reviewed the ways that the earthquake ground motion of shear waves affect a regional site with different site soil layers, and presents detailed analyses and explanations. Qian (1994) studied a site with a soft silt interlayer, and systematically summarized the factors affecting ground motion that had a response spectrum of acceleration with two marked spectrum peaks. Andrus and Stokoe (2000) carried out a simplified procedure using shear-wave velocity measurements to evaluate the liquefaction resistance of soils. Polito and Martin (2001) carried out cyclic triaxial tests to clarify the effects of nonplastic fines on the liquefaction susceptibility of sands. They suggested the need for further evaluation of the effects of nonplastic fines content upon penetration resistance, and the manner in which this relationship affects the simplified methods currently used in engineering practice to evaluate the liquefaction resistance of silty soils. Bo *et al.* (2003a, b) analyzed a large quantity of borehole data by computer program and probed of response spectrum and the peak value of accelerations. Boulanger and Idriss (2006) studied the new liquefaction susceptibility criteria for saturated silts and clays,

Correspondence to: Cui Jie, Earthquake Engineering Research & Test Center, Guangzhou University, Guangzhou 510405, China
Tel: +86-20-86575840; Fax: +86-20-86575840
E-mail: jcui2009@hotmail.com; lyd9999@163.com
†PhD; ‡Professor

Supported by: National Program on Key Basic Research Project (973 Program) under Grant No. 2011CB013606, Program for Changjiang Scholars and Innovative Research Team in University under Grant No. IRT13057, Key Program of National Natural Science Foundation of China under Grant No. 51438004 and the Research Fund for the Doctoral Program of Higher Education of China under Grant No. 20124410110004
Received JNovember 19, 2013; **Accepted** August 11, 2014

which are based on the mechanics of their stress-strain behavior and provided improved guidance for selecting engineering procedures to estimate potential strains and strength loss during seismic loading. Akhaveissy *et al*. (2009), Park and Desai (2000), Pradhan and Desai (2006) studied the cyclic behavior of saturated clays and clay-steel interfaces based on a disturbed state concept (DSC) model, which was used to predict field behavior of an instrumented pile subjected to cyclic loading. They then used a nonlinear dynamic finite-element program (DSC-DYN2D) with the DSC model to solve a typical boundary value problem–a shake table test involving liquefaction behavior and predicted stress-strain-pore water pressure behavior for the sand based on a comparison of the results from the DSC model and the test data.

Shaking table tests, as one important method to reproduce seismic sites at home and abroad, has been widely used in the field of dynamics and has been frequently used by researchers studying special site conditions. For example, Chen *et al.* (2007) carried out shaking table tests to study the interaction between the dynamic caused by soil and subway tunnels and also between the dynamic caused by soil in deep soft sites and underground structures of a subway. Tamura *et al.* (2000) carried out a large-scale test to study the interaction between liquefaction, soil and structures at the National Research Institute of Earth Science and Disaster Prevention. Li *et al.* (2008) carried out shaking table tests in the free field of liquefied foundations, which revealed the rules of dynamic interaction on liquefied site conditions. Ye *et al.* (2013) studied the growth and dissipation on excess pore water pressure in saturated sand by using pneumatic shaking table tests. Sadrekarimi (2013) carried out 1 g shaking table tests to study the dynamic behavior of granular soil at a shallow depth, thus showing that, with a reduction in effective confining stress. Srilatha *et al.* (2013) studied the effect of frequency on the seismic response to reinforced soil slopes by using shaking table tests, thus confirming that the effect of frequency on acceleration amplification is not powerful for reinforced slopes on all frequencies. Haeri *et al.* (2012) arrived at a conclusion that the behavior of pile groups without pile caps in an infinite mild slope far from a free face is different from that of the slope located behind a quay-wall or close to a free face, which was confirmed by other investigators using large-scale shaking table tests.

Previous investigations mainly focused on sites with either complex and uniform geological conditions or the interaction between soil and underground structures. Tests for site characteristics have been relatively rare. To find answers to the above-mentioned problems, the authors designed and completed a referential contrast test to determine the conditions for a regional site containing sand layers (Site II) and an all-clay site (Site I), thus exploring the effect of the change in the soil layer rigidity of soil layers on the dynamic characteristics of sites by changing the types and amplitudes of seismic wave input. In the test, data on the acceleration and pore water pressures in different positions of the model were measured, and Fourier transform was used to determine the acceleration. Thus, the rules including not only the changes in seismic amplification coefficient of different types of sites and in the effect of the liquefied layer on the level of the ground surface but also the amplitude of the vertical acceleration were established. Meanwhile, the effects of filter action of both sites on seismic waves of different frequencies as well as the relation between the natural frequency of the site ground surface and the amplitude of acceleration were analyzed. The authors also discovered the response mechanism and dynamic characteristics of the system of the site models containing sand layers under the seismic actions. Thus, the results can provide guidance for the design of aseismic buildings.

2 Design of shaking table test

2.1 Model system

The soil test chamber of a laminated shear-type model was designed based on achievements of existing model chamber development (Sun *et al.*, 2011), as shown in Fig. 1. Clay and sand were adopted as the geotechnical materials in the test chamber, the former being used to simulate the all-clay site (Site I), and the latter was backfilled by layer and compacted with a layering thickness of 15 cm. Table 1 shows the soil parameters of Site I after compaction. Clay with an interlayer of saturated sand was used to simulate the regional site (Site II). A static 10 cm water-head was placed for 24 hours in Site II, specifically in front of the clay and above the sand layer, to keep the sand layer saturated. The physical parameters of soil are shown in Table 1, and the sand grain composition is shown in Fig. 2.

Accelerometer (A) and pore water pressure sensor (K) were arranged in corresponding positions of the test system according to the test design and the combined research results of previous studies that identified the most vulnerable positions (Yang *et al.*, 2004). Figure 3 shows the final design and sensor arrangement of Sites I and II.

2.2 Loading case

The seismic waves of El Centro, referred to as El-C in the following table and figures, and Taft waves were used in the test. The one-way horizontal direction (X) and the two-way horizontal and vertical directions (X, Z), respectively X and Z, were adopted as input directions. The peak value of seismic waves input in the vertical direction was two-thirds of that in the horizontal direction. The acceleration peak values input were set as 0.1, 0.2, 0.4, and 0.6 g to determine the effect of

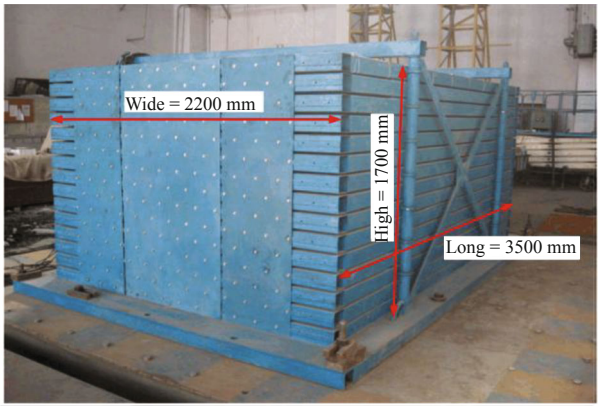

(a) Model box

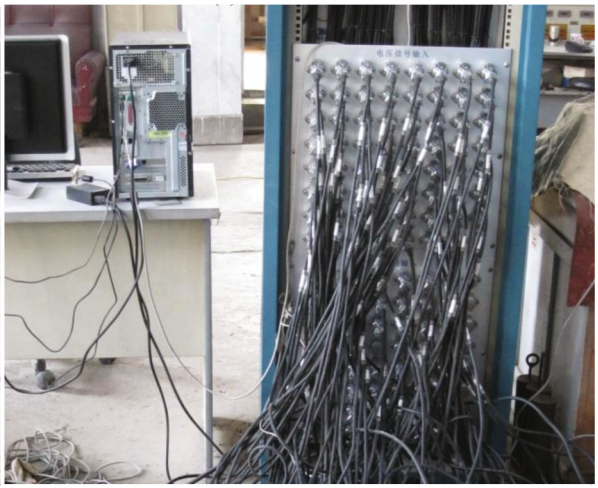

(b) Data acquisition system

(c) Water pressure monitoring system

Fig. 1 Model box and test system

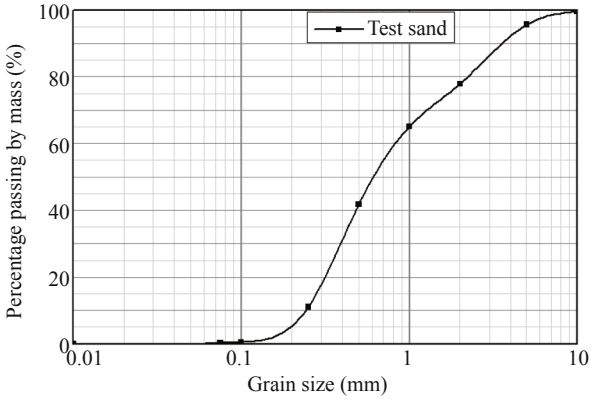

Fig. 2 Grain composition curve of sand

seismic amplitude on the sites. For Site I, scanning was performed by inputting 0.02 g of white noise after each loading. For Site II, loading was not performed again until the pore water pressure vanished completely after the last loading. The detailed loading case is shown in Table 2.

3 Results and analyses

3.1 Site liquefaction analyses

The pore water pressure of the liquescent saturated land layer surges because of seismic action. Therefore, site liquefaction can be reflected through the changes in the pore water pressure of the site. The pore water pressure sensor (K1) was installed on the site shown Fig. 3 to monitor the pore water pressure of the sand layer. Figure 4 shows the time-history curve of the pore water pressure under the action of each magnitude of the E1 Centro and Taft waves.

The data in Fig. 4 show that the pore pressure caused by different seismic waves and different loading only produced a wave motion within a narrow range at the early stage of the test, in a time-history of 0 to 6 s, and no pore pressure accumulation was found. At the middle stage of the test, approximately in 3 s to 12 s, the pore pressure accumulated radically and reached the peak. After reaching the peak, the pore pressure remained unchanged at the later stage of the test, in 10 s to 15 s, and a slight decline was observed. Figure 6 shows the relationship between pore pressure peak and acceleration under each test condition shown in Fig. 7.

Table 1 Soil parameters of sites

Soil	Density (g/cm^3)	Site shear wave velocity (m/s)	Moisture content (%)	Plastic index, I_p
Clay I	1.89	237.5	27.8	16
Sand	2.16	183.4	—	—
Clay II	2.01	221.8	36.4	20

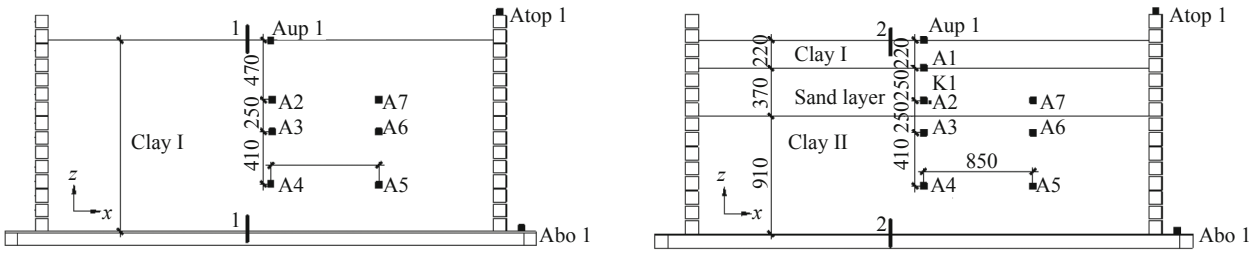

(a) Complete clay site (Site I) (b) Regional site with one sand layer (Site II)

Fig. 3 Structural conditions of sites and layout of sensors

Table 2 Loading case

Loading sequence	Loading cases	Sites
1, 2	0.1 g El-C (*X*, *XZ*)	I, II
3, 4	0.1 g Taft (*X*, *XZ*)	I, II
5, 6	0.2 g El-C (*X*, *XZ*)	I, II
7, 8	0.2 g Taft (*X*, *XZ*)	I, II
9, 10	0.4 g El-C (*X*, *XZ*)	I, II
11, 12	0.4 g Taft (*X*, *XZ*)	I, II
13, 14	0.6 g El-C (*X*, *XZ*)	I, II
15, 16	0.6 g Taft (*X*, *XZ*)	I, II

Note: 1. The loading case did not include the white-noise loading cases;
2. The "*X*, *XZ*" in loading cases were action directions;
3. The "*X*" direction loading case was taken first.

The data in Fig. 6 show that the pore water pressure of the sand layer initially increases and subsequently decreases with the load acceleration peak increasing from 0.1 g to 0.6 g. Specifically, under the 0.4 g test condition, the pressure reaches the maximum value of 0.602 kPa under the action of 0.4 g E1-C-*X*. When the acceleration peak reached 0.6 g, the pore pressure did not increase accordingly but decreases drastically. Seismic waves are introduced to the soil layer at the early stage of the test. However, the stress transmission medium and the stress distribution form do not change significantly because of the failure of vibration and dislocation of the sand grains in the sand layer. Therefore, the pore pressure does not significantly increase. At the middle stage of the test, the sand grains are compacted and the stress is mainly taken

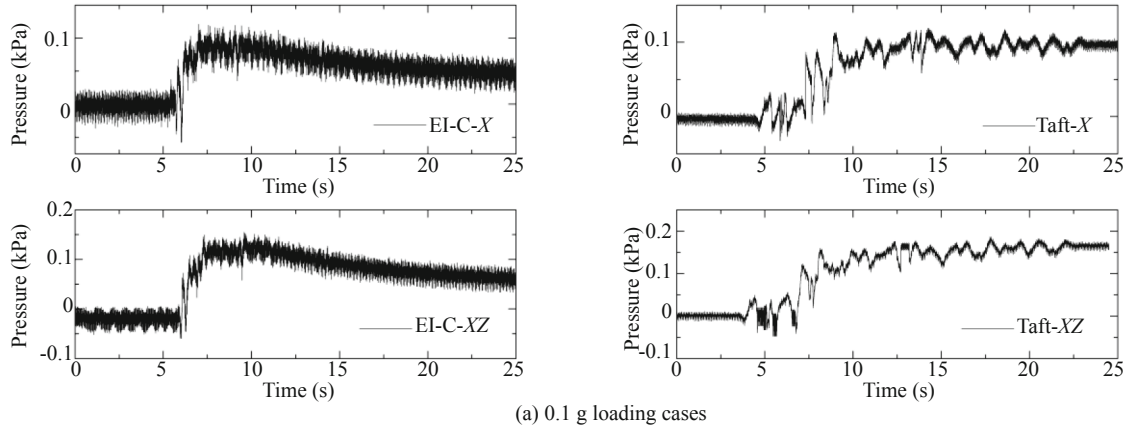

(a) 0.1 g loading cases

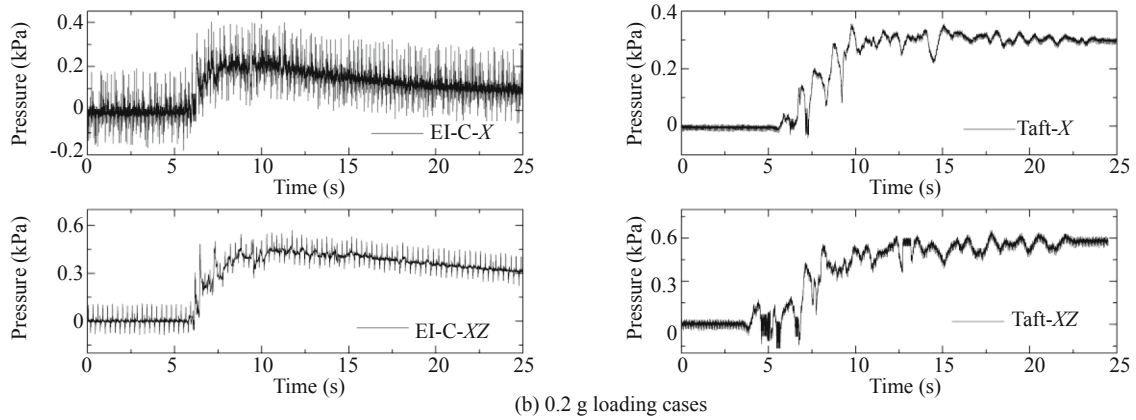

(b) 0.2 g loading cases

Fig. 4 Pore water pressure time history at K1

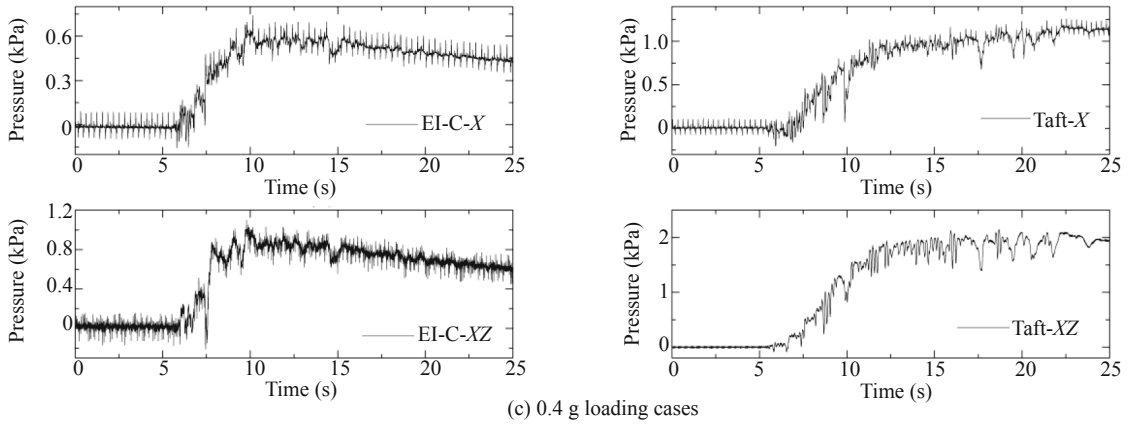

(c) 0.4 g loading cases

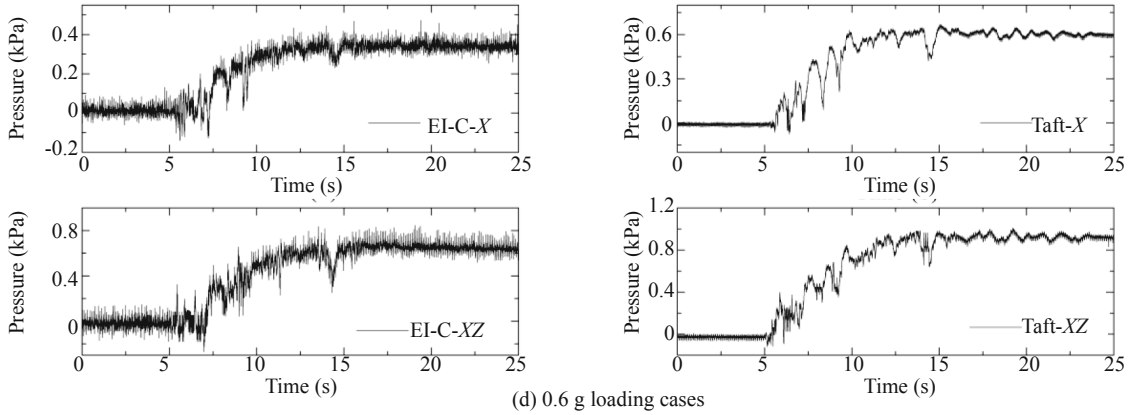

(d) 0.6 g loading cases

(Note: the legend El-C means El Centro seismic action)

Fig. 4 Continued

Fig. 5 Surface phenomena after the 0.4 g Taft-*XZ* loading case

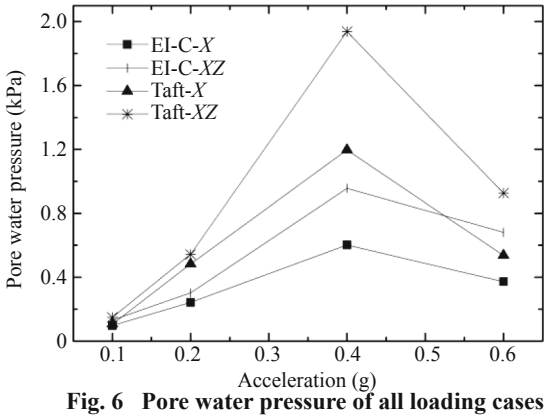

Fig. 6 Pore water pressure of all loading cases

by water because of vibration and dislocation. Thus, the pore pressure increases abruptly within a very short time. On the basis of the principle of effective stress, sand has been liquefied at this moment. Liquefaction is observed in the test, and water is emitted from the sand layer. Water was present on the surface layer of the site, as shown in Fig. 5. At the later stage of the test, the sand was completely liquefied, and the effective stress is zero. The load of the soil is completely transferred by the pore pressure. As the test continues, the water from the sands is transferred to the upper clay, and the sand grains recombine. Thus, the pore water pressure remains unchanged or drops slightly at this stage.

The ratio of the response peaks of the pore pressure

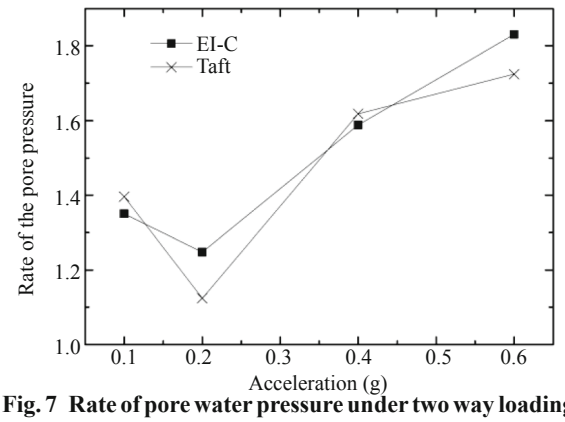

Fig. 7 Rate of pore water pressure under two way loading cases

from the two-way and one-way excitation under the same seismic waves are shown in Fig. 7, from which it is known that, under the action of E1 Centro waves, the maximum response of the sand layer pore pressure under the two-way transmission is 1.27 to 1.83 times that under the one-way transmission. By comparison, under the action of Taft waves, the maximum response of the sand layer pore pressure under the two-way transmission is 1.11 to 1.69 times that under the one-way transmission. The two-way seismic waves have a greater effect on site liquefaction than the one-way seismic waves. Moreover, the maximum pore pressure increment of the site is 0.950 kPa under the action of E1 Centro-*XZ* waves, but 1.931 kPa under the action of Taft-*XZ* waves. Compared with E1 Centro waves, the greater amplitude of Taft-*XZ* waves lasts longer; that is, the oscillating seismic excitation to site liquefaction is more apparent.

3.2 Analyses of site acceleration

3.2.1 Time-history and amplification factor of site acceleration

The time-history curves of the *X* and *Z* directions at Aup1 on the surface of Sites I and II under the load conditions of 0.1 and 0.6 g E1 Centro waves are shown in Fig. 8, from which it is seen that the acceleration peak measured under each condition of Site II is smaller than that under each condition in Site I. To analyze the effect of sites on seismic amplitude, the acceleration amplification factor is defined as the ratio of the maximum acceleration amplitude measured in the position to the input seismic amplitude. The amplification factor of acceleration in the *X* direction of the surface is shown in Fig. 9, which shows that the maximum amplification factors of two sites both appear in the position of 0.1 g amplitude. The amplification factor of the surface acceleration on Site I decreases as the input acceleration peak of the seismic waves increase and is greater than 1. The amplification factor of acceleration on Site II is smaller than that of Site I under the same condition, and the inflection point appears in the position of 0.4 g amplitude. The minimum value of the corresponding amplification factor is 0.813. Comparing Fig. 9(a) with Fig. 9(b), the amplification factor of the acceleration obtained under two-way excitation is slightly greater than that obtained under one-way excitation. Analytical results show that the site is denser under the action of a vertical earthquake, and the vertical earthquake interferes with the spread of the horizontal earthquake.

3.2.2 Acceleration amplification factor in different positions

Figure 10 shows the ratio of the acceleration amplification factor of Aup1 in Site II (surface) to that in Site I under the same conditions. The ratio is smaller than 1, which indicates that Site II has a smaller effect on seismic amplification compared with Site I.

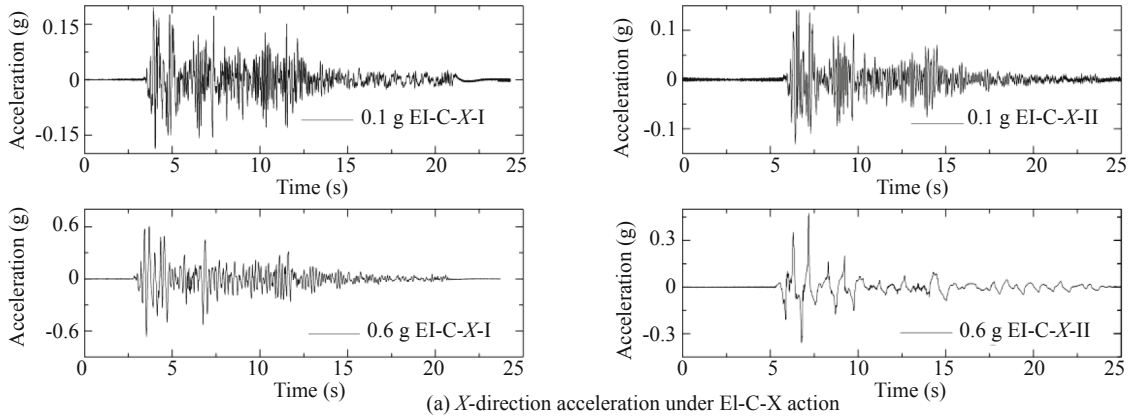

(a) *X*-direction acceleration under El-C-X action

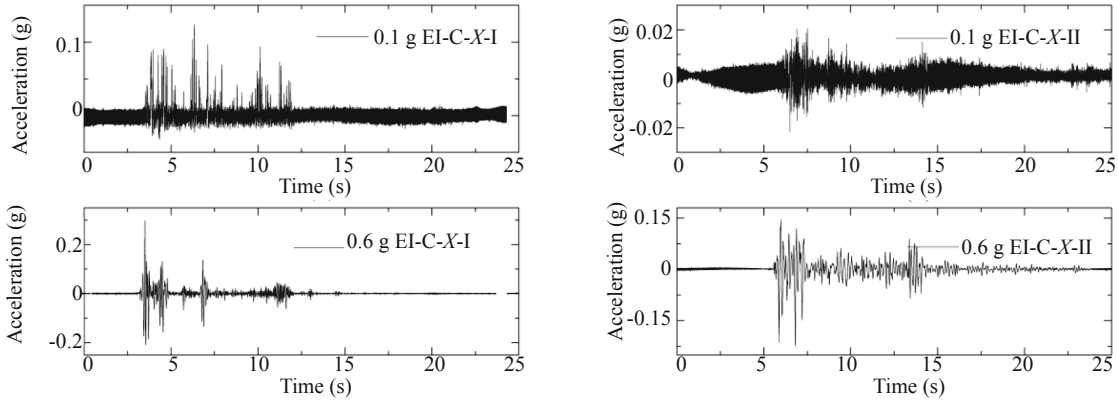

(b) *Z*-direction acceleration under El-C-*X* action

Fig. 8 Acceleration time history at Aup1 under 0.1 and 0.6 g amplitude loading case

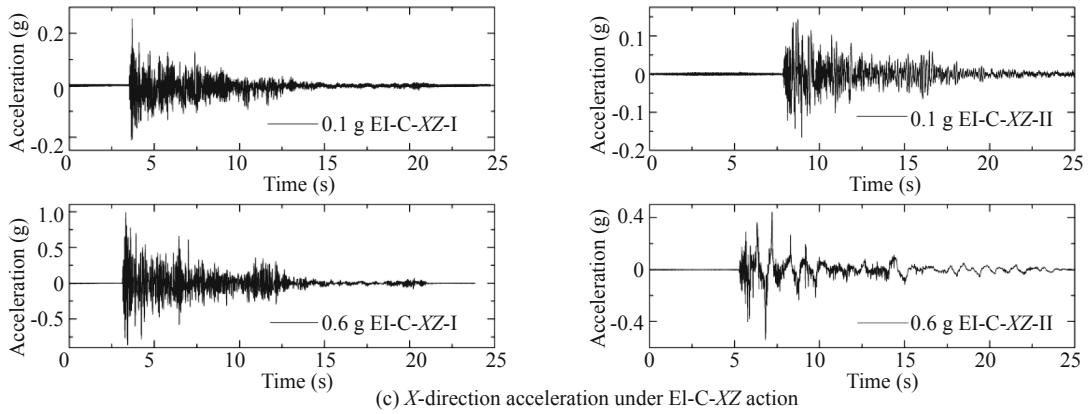

(c) *X*-direction acceleration under El-C-*XZ* action

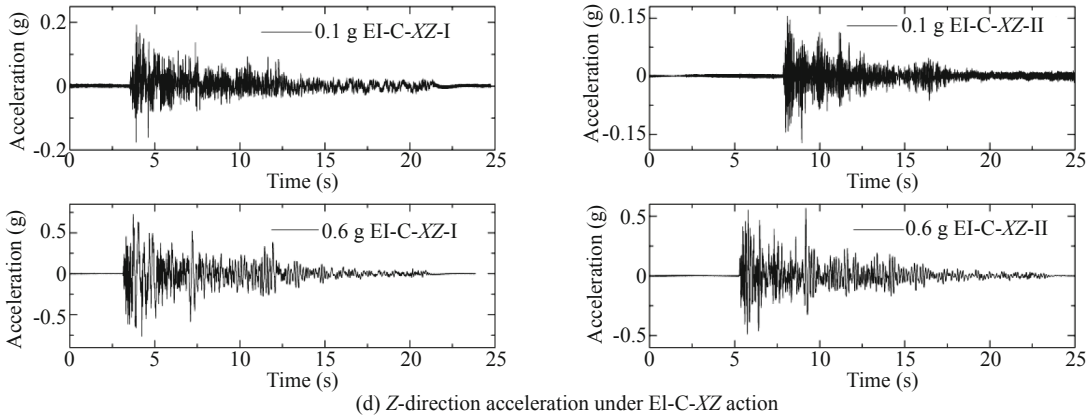

(d) *Z*-direction acceleration under El-C-*XZ* action
(Note: the legend El-C means El Centro seismic action)

Fig. 8 Continued

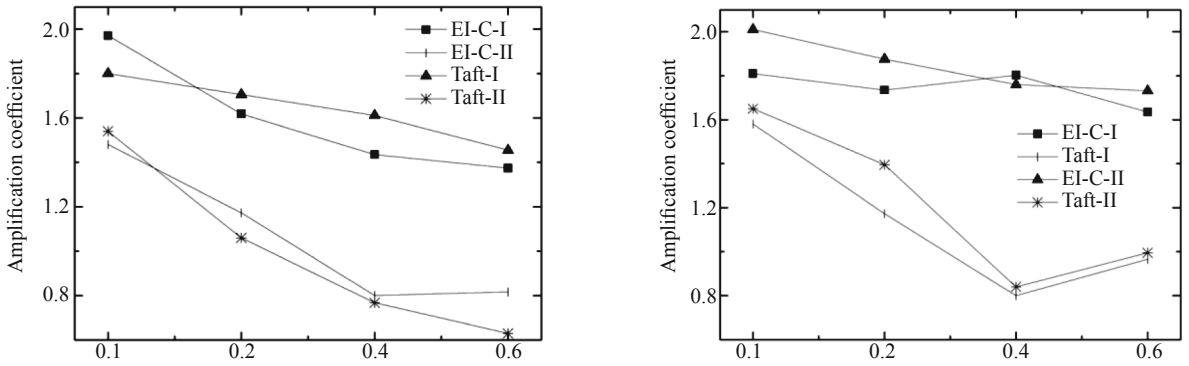

(a) One-way excitation (b) Two-way excitation

Fig. 9 Amplification coefficients of Aup1 under loading case

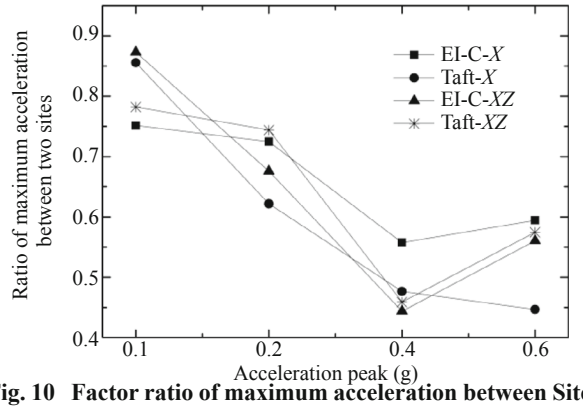

Fig. 10 Factor ratio of maximum acceleration between Site II and Site I at Aup1

In Fig. 11, the acceleration amplification factors of the basements the two sites show are estimated at 1.0 to 1.2 under the action of E1 Centro seismic waves. The 1-1 section is for Site I, and the 2-2 section is for Site II, as seen in Fig. 3.

Figure 11 shows that, under the action of one-way excitation, the acceleration amplification factors of the two sites on the basement range from 1.0 to 1.2 and are approximately equal. The conclusions derived from the slope change of the fold line in Fig. 11 are as follows. Site I can magnify the earthquake excitation, and the amplification rate decreases as the acceleration amplitude increases; as a whole, the acceleration amplification

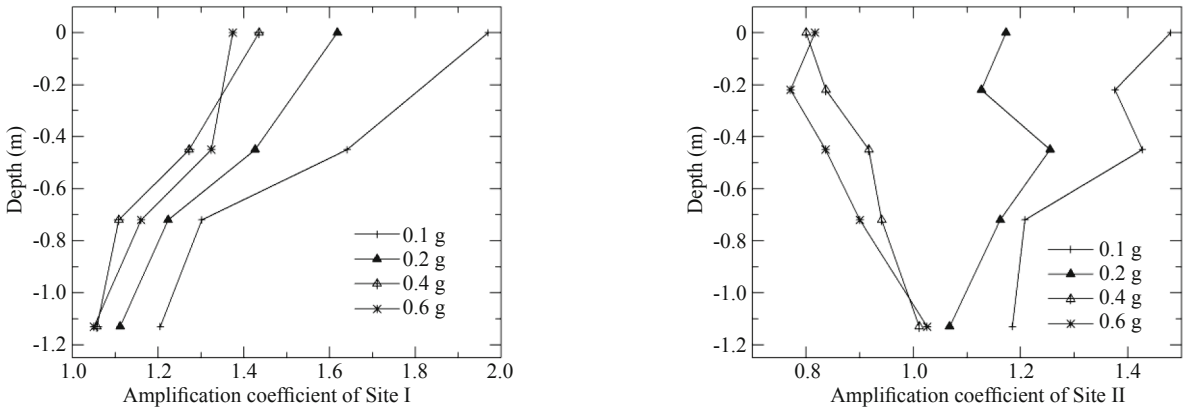

Fig. 11 Factor ratio of maximum acceleration between Site II and Site I

factor of Site II decreases under the condition of 0.4 and 0.6 g amplitudes and increases under the condition of 0.1 and 0.2 g. As the seismic wave transfers towards the surface, the amplification factor of Site I increases, the amplification factors of Site II decreases at a depth range of -0.44 m to -0.22 m under the conditions of 0.1 and 0.2 g, and the maximum decreased amplitude is estimated at 0.2 g; from 1.201 g to 1.093 g, the amplitude reaches 8.99%.

The all-clay site can amplify the seismic wave amplitude. The acceleration amplification factor decreases as the input seismic amplitude increases and increases with the upward transmission of seismic waves. The regional site has a smaller contribution to the amplification of the seismic amplitude compared with the all-clay site. Under 0.4 g two-way excitation, the acceleration amplification factor ratio reaches the minimum value of 0.451, as seen in Fig. 10. In the regional site, the small-amplitude seismic condition has an amplifying effect, and the great-amplitude excitation has a gradually decreasing effect on the seismic amplitude. It has been proved from the above analyses that the sand layer of the regional site is liquefied under the 0.4 g strong oscillation excitation, which directly affects the amplitude of the seismic waves measured after passing the site.

The possible reasons for this phenomenon are explained as follows. (Li *et al.*, 1992). The soil was turbid liquid with dense grains after the liquefaction of strong vibration, and the shear strength is different from that in the previous site. Under strong vibration, the clay under the sand layer is softened and the dynamic properties change. The surrounding containers and the soil around the liquefaction area affect the soil near the sensor, and the viscosity and shear of the water affect the seismic waves.

3.3 Analyses of site spectrum

The frequency components contained in the process of seismic wave time can be obtained by means of Fourier spectrum (Ohsaki, 2008). To discuss the dynamic properties of the sites, Fourier transform of the measured acceleration time-history should be performed. Figure 12 presents the Fourier spectrum for the acceleration in the *X* direction of the two sites at the Aup1 position under the one-way action of E1 Centro seismic waves. Figure 13 presents the Fourier spectrum in the *X* and *Z* directions at Aup1 under 0.6g two-way excitation.

Figure 12 indicates that the one-way excitation amplitude of El Centro seismic waves increases from 0.1 g to 0.6 g. Moreover, the natural frequency of the Site I surface decreases from 11.027 Hz to 3.202 Hz, and the natural frequency of the Site II surface gradually decreases from 6.866 Hz to 1.184 Hz. In Site II, under the two-way excitation, the natural frequency in the *Z* direction is greater than that in the *X* direction, and ranges from 5.092 Hz to 11.89 Hz.

Figure 14 shows that the maximum natural frequency of two sites under each condition appears at 0.1 g acceleration amplitude, and the minimum value corresponds to 0.6 g acceleration amplitude. The natural frequency of Site II is less than that of Site I. Figure 15 shows the relationship ratio of both sites.

It is seen from the analyses of all Fourier spectra of site acceleration that the site plasticity changes as the acceleration amplitude increases under seismic excitation and filtration on the high-frequency section. The amplification on the low frequency section is more significant, and under seismic action in the regional site, the saturated clay is softened and the saturated sands are liquefied. Thus, the change of site rigidity is small and the site quality is unchanged. The characteristic frequency in the regional site is smaller and was 0.239 to 0.637 times that of the all-clay site. As shown in Fig. 15, under two-way excitation, the natural frequency of Site II is 0.239 times that of Site I. Figure 16 shows that the natural frequency of each site gradually decreases during the seismic wave transmission. Thus, the regional site shows a seismic-reducing effect on structures with shorter natural vibration periods but showed a seismic-strengthening effect on structures with longer natural vibration periods.

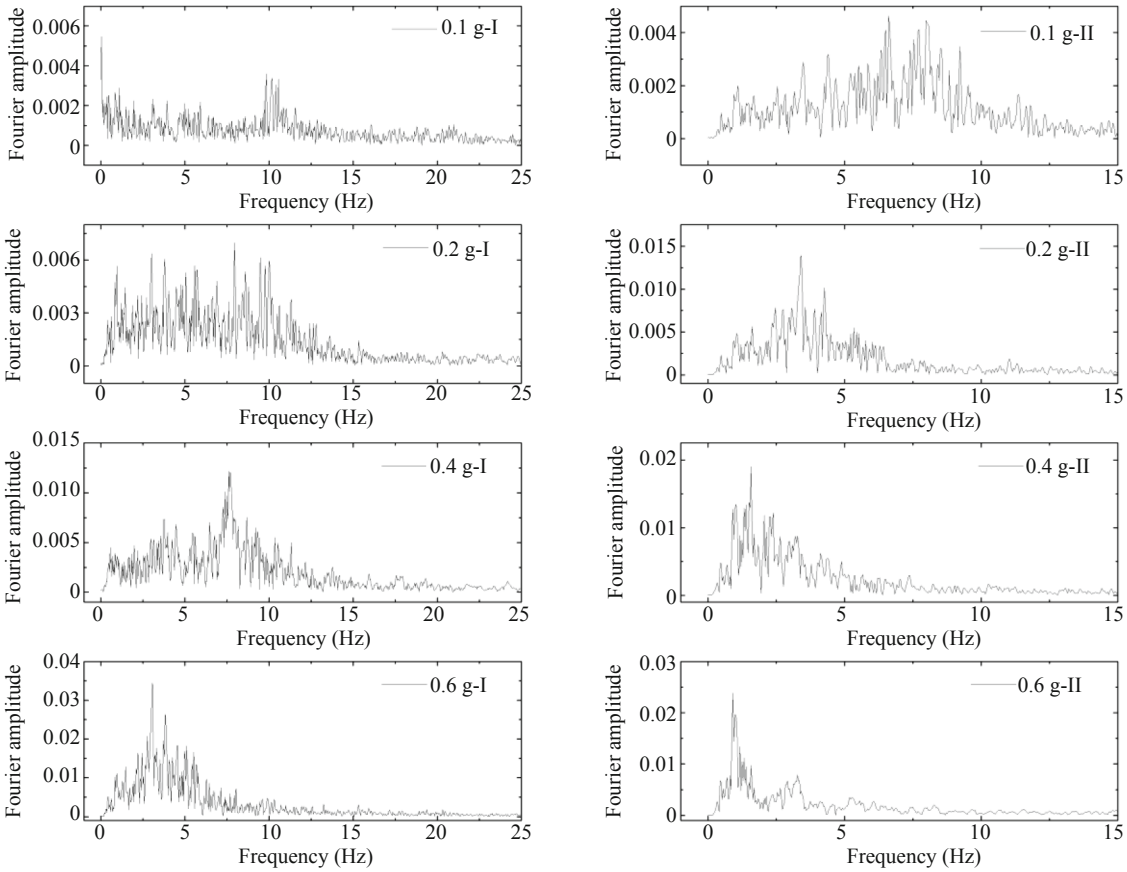

Fig. 12 Acceleration FFT at Aup1 in two sites under El-C wave

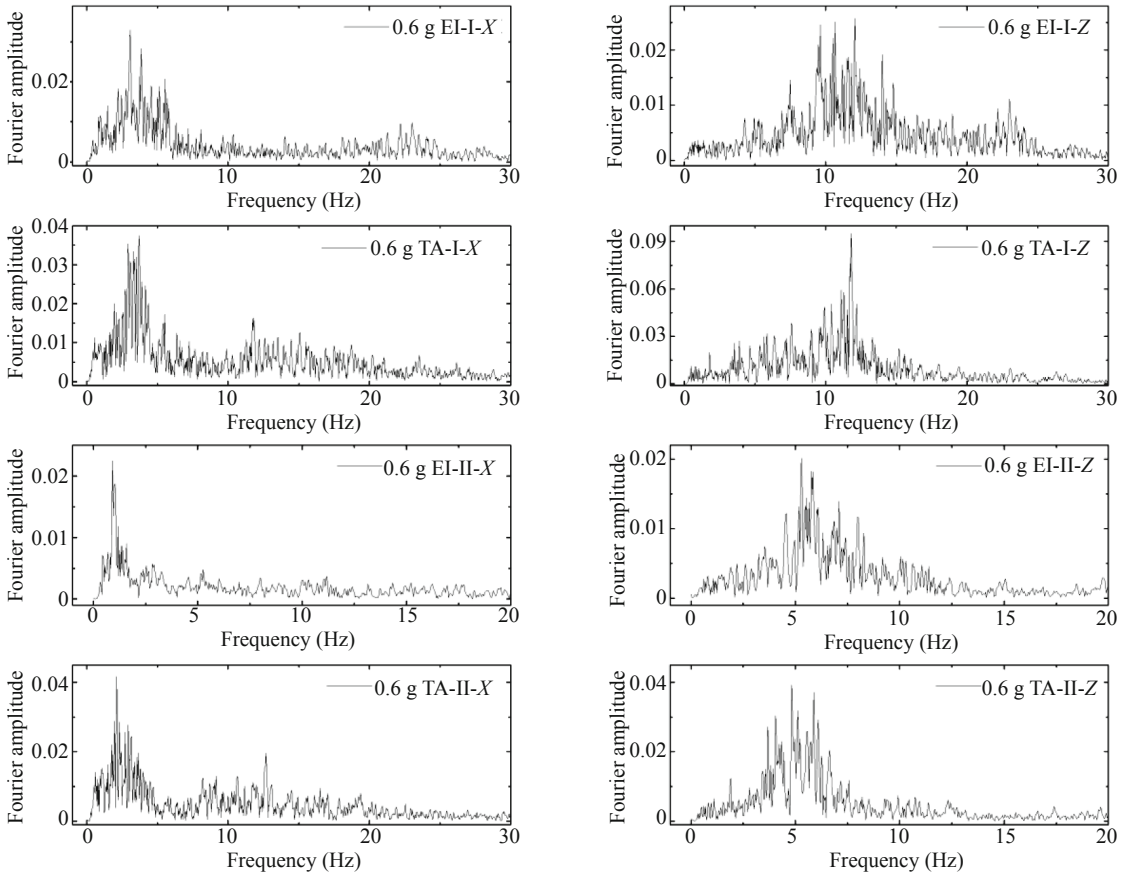

Fig. 13 *X*, *Z* direction acceleration FFT at Aup1 under bidirectional earthquake wave

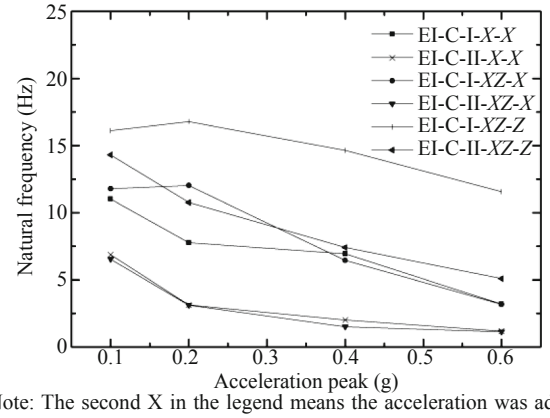

(Note: The second X in the legend means the acceleration was adopted in the *X* direction.)

Fig. 14 Natural frequency of Aup1 under El-C case

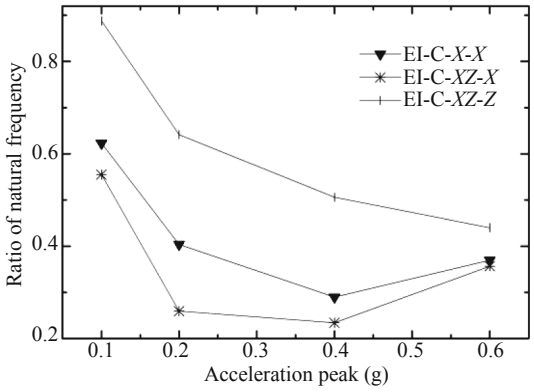

Fig. 15 Ratio of Aup1 natural frequency between Site II and Site I

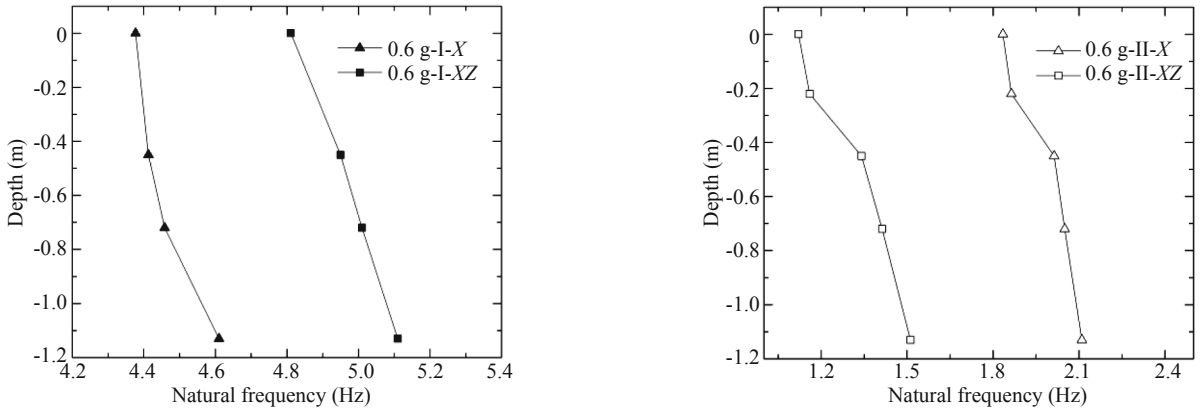

Fig. 16 Natural frequency of Aup1 under El-C case

4 Conclusions

On the basis of the shaking table tests under all-clay and regional site conditions, the dynamic response rules in terms of site acceleration response, pore water pressure, and Fourier spectrum, are analyzed. The following conclusions are drawn.

(1) With the increase in seismic wave amplitude, the pore water pressure of the sand layer in the regional site initially increases and subsequently decreases, and the seismic wave amplitude corresponding to the pore pressure peak is 0.4 g. The pore water pressure under two-way load conditions increases by 10% to 83%, compared with that under one-way load conditions. The oscillating seismic waves have a significant liquefaction effect on the sites.

(2) The all-clay site increases the seismic amplitude, and its amplification on the acceleration amplitude weakens with the increase in acceleration amplitude and increases with the transmission of seismic waves towards the surface. Bidirectional seismic motion promotes the acceleration amplitude, with the maximum amplification factor of 1.96 under the 0.6 g two-way excitation. As the input seismic amplitude increases, the natural frequency of vibration obtained from the seismic waves passing the complete clay layer decreases from 11.027 Hz to 3.202 Hz. Apparently, the effect of sites on high-frequency filtration and the low-frequency amplification of seismic waves becomes even more prominent.

(3) The acceleration amplification factor in the regional site is 0.451 to 0.881 times that in the all-clay site, its corresponding value being the minimum under 0.4 g two-way excitation. Sites can amplify the seismic amplitude under low amplitude seismic action of 0.1 and 0.2 g. By comparison, under high seismic excitation of 0.4 and 0.6 g, sand liquefaction and clay softening decrease the amplification factor, thus resulting in significant seismic reduction. After the seismic waves pass the sand layer of the regional site, the acceleration amplitude decreases, and 0.2 g corresponds to the greatest amplitude decrease of 8.99%.

(4) Compared with the all-clay site, the regional site has a smaller natural frequency of vibration, but has a more powerful effect on the filtration of high frequency and the amplification of low frequency. The natural frequency of vibration in the *X* direction of the regional site is 0.239 to 0.637 times that of the all-clay site; its minimum value was acquired under 0.4 g two-way excitation. With the transmission of seismic waves toward the surface, the natural frequency of vibration in each layer site gradually decreased. Therefore, the regional site can effectively reduce the seismic action

on short-periodic structures, but can enhance the seismic action on long-periodic structures.

Under 0.6 g excitation, the pore pressure is higher, and the natural frequency of vibration in the site is lower than those under 0.4 g excitation. Theoretically, this is because the sand layer has been liquefied and the sand particles have been redistributed by compaction under 0.4 g test conditions in the same test.

Acknowledgement

This study is financially supported by National Program on Key Basic Research Project (973 Program) (No. 2011CB013606), Program for Changjiang Scholars and Innovative Research Team in University (No. IRT13057), Key Program of National Natural Science Foundation of China (No. 51438004) and the Research Fund for the Doctoral Program of Higher Education of China (No. 20124410110004). The authors express sincere thanks to Ph.D. Haifeng Sun, Ph.D. Haian Liang, Mr. Xianchun Meng, Mr. Yan Zou and Mr. Chunhui Liu for assisting in preparation of this manuscript.

References

Akhaveissy AH, Desai CS, Sadrnejad SA and Shakib H (2009), "Implementation and Comparison of a Generalized Plasticity and Disturbed State Concept for the Load-deformation Behavior of Foundations," *Scientia Iranica Transaction A-Civil Engineering*, **16**(3): 189–198.

Andrus RD and Stokoe KH (2000), "Liquefaction Resistance of Soils from Shear-wave Velocity," *Journal of Geotechnical and Geoenvironmental Engineering*, **126**(11): 1015–1025.

Bo Jingshan, Li Xiulin and Liu Hongshuai (2003a), "Effects of Soil Layer Construction on Peak Accelerations of Ground Motions," *Earthquake Engineer and Engineering Vibration*, **23**(3): 35–40. (in Chinese)

Bo Jingshan, Li Xiulin, Liu Dedong and Liu Hongshuai (2003b), "Effects of Soil Layer Construction on Characteristic Periods of Response Spectra," *Earthquake Engineering and Engineering Vibration*, **23**(5): 42–45. (in Chinese)

Boulanger RW and Idriss IM (2006), "Liquefaction Susceptibility Criteria for Silts and Clays," *Journal of Geotechnical and Geoenvironmental Engineering*, **132**(11): 1413–1426.

Chen Guoxing, Zhuang Haiyang, Du Xiuli, Li Liang and Chen Shaoge (2007), "A Large-scale Shaking Table Test for Dynamic Soil-metro Tunnel Interaction: Analysis of Test Results," *Earthquake Engineer and Engineering Vibration*, **27**(1): 164–170. (in Chinese)

Haeria SM, Kavanda A, Rahmanib I and Torabia H (2012) "Response of a Group of Piles to Liquefaction-induced Lateral Spreading by Large Scale Shake Table Testing," *Soil Dynamics and Earthquake Engineering*, **38**: 25–45.

Li Peizhen, Ren Hongmei, Lv Xilin and Chenlei (2008), "Shaking Table Test on Free Field Considering Soil Liquefaction," *Earthquake Engineering and Engineering Vibration*, **28**(2): 171–178. (in Chinese)

Li Xiaojun (1992), "Analysis Method of Ground Earthquake Motion Affected by the Site Soil Layer," *World Earthquake Engineering*, **8**(2): 49–60. (in Chinese)

Li Xuening, Liu Huishan, Zhou Genshou and Wang Shifeng (1992), "Study on Shake-reducing Effect on Liquefiable Layers," *Earthquake Engineering and Engineering Vibration*, **12**(3): 85–91. (in Chinese)

Ohsaki Y (2008), *Introduction to the Spectral Analysis of Ground Motion*, Translated by Tian Qi, Beijing: Earthquake Press, 49–61. (in Chinese)

Park IJ and Desai CS (2000), "Cyclic Behavior and Liquefaction of Sand Using Disturbed State Concept," *Journal of Geotechnical and Geoenvironmental Engineering*, **126**(9): 834–846.

Polito CP and Martin JR (2001), "Effects of Nonplastic Fines on the Liquefaction Resistance of Sands," *Journal of Geotechnical and Geoenvironmental Engineering*, **127**(5): 408–415.

Pradhan SK and Desai CS (2006), "DSC Model for Soil and Interface Including Liquefaction and Prediction of Centrifuge Test," *Journal of Geotechnical and Geoenvironmental Engineering*, **132**(2): 214–222.

Qian Shenguo (1994), "A Study on Earthquake Response Properties of Soil with Weak Intercalation," *Earthquake Resistant Engineering*, **1**: 32–36. (in Chinese)

Sadrekarimia A (2013), "Dynamic Behavior of Granular Soils at Shallow Depths from 1 g Shaking Table Tests," *Journal of Earthquake Engineering*, **17**(2): 227–252.

Srilathaa N, Madhavi LG and Puttappac CG (2013), "Effect of Frequency on Seismic Response of Reinforced Soil Slopes in Shaking Table Rests," *Geotextiles and Geomembranes*, **36**: 27–32.

Sun Haifeng, Jing Liping, Wang Ningwei and Meng Xianchun (2011), "Development of Multifunctional Laminar Shear Container for Shaking Table Test," *Chinese Journal of Rock Mechanics and Engineering*, **30**(12): 2498–2506. (in Chinese)

Tamura S, Suzuki Y, Tsuchiya T *et al*. (2000), "Dynamic Response and Failure Mechanisms of a Pile Foundation during Soil Liquefaction by Shaking Table Test with a Large-scale Laminar Shear Box," *Proc. of 12WCEE*, New Zealand, 167–175.

Yang Linde, Ji Qianqian, Yang Chao and Zheng Yonglai (2004) "Optimization of Positions of Sensors in Shaking Table Test for Subway Station Structure in Soft Soil," *Rock and Soil Mechanics*, **25**(4): 619–623. (in Chinese)

Ye B, Ye GL, Ye WM and Zhang F (2013), "A Pneumatic Shaking Table and Its Application to a Liquefaction Test on Saturated Sand," *Natural Hazards*, **66**(2): 375–388.